



Thrust Force-Based Tool Wear Estimation Using Discrete Wavelet Transformation and Artificial Neural Network in CFRP Drilling

Chengwen Han¹ · Kyeong Bin Kim¹ · Seok Woo Lee² · Martin Byung-Guk Jun³ · Young Hun Jeong^{1,4}

Received: 16 September 2020 / Revised: 5 June 2021 / Accepted: 20 June 2021 / Published online: 19 July 2021
© Korean Society for Precision Engineering 2021

Abstract

Currently, carbon fiber-reinforced plastic (CFRP) is a material with potential uses for various industries due to its excellent properties. However, the severe tool wear in its machining is an evitable problem because it deteriorates product quality and productivity at the same time. Timely replacement of the tool should be taken in advance to reduce the influences of this drawback. In sum, the accurate estimation of the tool wear plays a crucial role in CFRP machining. Therefore, in this study, a tool wear estimation in CFRP drilling is presented. The method used is based on discrete wavelet transformation (DWT) of the thrust force signal and an artificial neural network (ANN). Two valuable features related to tool wear are identified and then extracted using DWT. The tool wear is estimated by using an ANN with two features adapted from DWT. Consequently, the tool wear, especially flank wear, in CFRP drilling can be accurately estimated using the proposed method.

Keywords Carbon fiber-reinforced plastic (CFRP) · Drilling · Tool wear · Thrust force · Discrete wavelet transformation (DWT) · Artificial neural network (ANN)

1 Introduction

The need for lightweight materials is drastically increasing, given the current industry trend for higher fuel efficiency and

environment protection. In particular, lightweight materials with higher toughness and strength can play more crucial roles in transportation system industries. Carbon fiber-reinforced plastic (CFRP) is a polymer-matrix composite (PMM), which is composed of a thermoset polymer matrix and carbon fiber reinforcement. CFRP has great potential for fair price and exhibits excellent properties such as high modulus, high strength, low density, and good resistance to corrosion [1–3]. Thus, CFRP is a promising material used in innovating transportation systems, especially with automobile [2, 4] and aerospace applications [1–3, 5–7].

In spite of the large demand for CFRP, several issues remain concerning its recycling properties [8], price [9], and machining [2]. CFRP machining is difficult to solve. Thus, proper selection of the cutting tool is important and the optimal cutting condition should always be considered when machining CFRP, given its material discontinuity, inhomogeneity, and anisotropic nature [2, 10, 11]. Moreover, unlike conventional metals, machining CFRP is accompanied with excessive tool wear, which is based on the abrasive nature of the wear [11, 12]. This tool wear can also result in several types of damages on CFRP [12–16], including fiber pull-out, matrix cracking, thermal damage, and delamination [14, 17, 18]. Particularly, delamination is the one of the most severe and frequent failures in CFRP drilling. Lin et al. investigated

✉ Young Hun Jeong
yhjeong@knu.ac.kr

Chengwen Han
531295911@qq.com

Kyeong Bin Kim
kkb4615@gmail.com

Seok Woo Lee
swlee@kitech.re.kr

Martin Byung-Guk Jun
mbgjun@purdue.edu

¹ Department of Mechanical Engineering, Kyungpook National University, 80 Daehakro, Bukgu, Daegu 41566, Republic of Korea

² Dongnam Regional Division, Korea Institute of Industrial Technology, 804 Baegyong-daero, Sasangu, Busan 46938, Republic of Korea

³ School of Mechanical Engineering, Purdue University, 585 Purdue Mall, West Lafayette, IN 47907-2088, USA

⁴ School of Mechanical Engineering, Kyungpook National University, 80 Daehakro, Bukgu, Daegu 41566, Republic of Korea

the nature of delamination in CFRP and concluded that the tool wear is a major factor that increases the occurrence of delamination [19]. However, Hou et al. presented that introduction of external cooling lubricant to CFRP drilling process could reduce the tool wear and improve the machined surface quality [20]. Mura and Dini proposed that the pre-cooling treatment by cryogenic fluid could reduce the delamination of CFRP and improve the machined surface quality even though the tool wear was accelerated [21].

Tool condition monitoring (TCM) [22] is one of the most important technologies for autonomous and unmanned manufacturing systems. TCM can alleviate the problems induced by tool wear in CFRP drilling. Although studies on tool wear monitoring in metal drilling are frequent [22–24], investigations on tool wear monitoring in CFRP (or even GFRP) drilling are not yet popular. In particular, only a few have been reported. Caggiano and Nele have proposed a tool wear estimation based on an artificial neural network (ANN) with sensor fusion in drilling CFRP [25]. Al-Sulaiman et al. examined the relationship between electrical power and tool wear in CFRP drilling for TCM [26]. Studies on the influence of tool wear on thrust force was also conducted [12, 13, 27, 28] because thrust force is one of the most sensitive signals to tool wear. Acoustic emission has been frequently considered a practical and potential signal to indicate tool wear in drilling fiber-reinforced composites [29]. Zhu et al. presented that ANN based on thrust force and acceleration signals could successfully identify the tool state [30]. Although strong correlation exists between tool wear and sensor signals, most of the signals cannot effectively indicate the wear directly due to the noise or interference from the machining process and environment. Therefore, various signal processing methods, which extract meaningful information from the raw signal, have been applied to tool wear monitoring, including the following exemplary methods: statistical parameters, auto regressive moving average, fast Fourier transformation (FFT), and wavelet transformation [23].

In this study, we present a tool wear estimation in CFRP drilling using only thrust force signal, which possesses lots of valuable information related to the quality of drilling process such as tool condition and delamination [14, 27, 28]. Specifically, the quasi-static (low frequency) and dynamic (2nd harmonic of runout frequency) components of the thrust force signal are extracted using discrete wavelet transformation (DWT) for a fast and efficient process. Then, these two features are independently provided to decision making based on an ANN to accurately estimate the tool wear. Consequently, the tool wear in CFRP drilling could be successfully estimated with the help of the independent consideration of the two given frequency components of thrust force signal in DWT and ANN. Furthermore, the independent consideration of the two given frequency components could improve the estimation accuracy and reliability from the typical way according to the consideration of the quasi-static component.

2 Methods of Flank Wear Estimation

2.1 Concept of Tool Wear Estimation

Figure 1 shows the proposed procedure of tool wear estimation for CFRP drilling. Estimation of tool wear in this study consists of three steps, namely, signal measurement, signal processing, and estimation. In this study, the thrust force is regarded as the physical signal that estimates the tool wear. This physical signal can be measured using a tool dynamometer through analog-to-digital conversion (ADC). Since the tool wear affects the average level and fluctuation behavior of the cutting forces [31, 32], the quasi-static and dynamic components are extracted from the signal in this study. The quasi-static component can cover the cutting force increase induced by the tool wear, whereas the dynamic component corresponds to the vibration rise caused by the tool wear. These components can be obtained using various methods such as FFT, time series analysis, statistics, and wavelet transformation [23]. In this study, DWT is employed because it has useful properties for tool condition monitoring [33, 34]. With the help of DWT, signal decomposition to the quasi-static and dynamic components can be achieved along with denoising effect, which removes the meaningless parts and extracts more meaningful ones. The extracted two components are considered the independent features in tool wear estimation in the proposed method. ANN is used to estimate tool wear in CFRP drilling from the extracted two features (i.e., components) with higher accuracy.

2.2 DWT

Wavelet transformation is a method used to decompose a signal into components with different resolution levels [35].

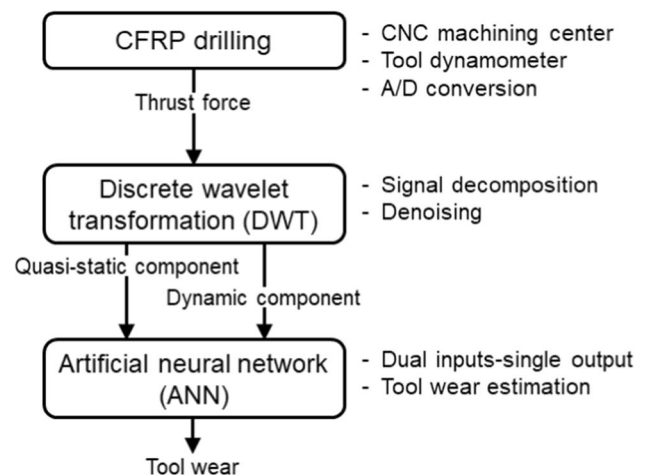


Fig. 1 Schematics of tool wear estimation for CFRP drilling

This method’s capability of correlating the signal with a family of waveforms concentrated in time and in frequency is considered as its advantage [34]. In particular, DWT is based on the discrete signal, and thus it is appropriate to the signal uniformly sampled at an interval. In this study, Daubechies (*Daub4*) wavelet transformation is used [35]. It has four *scaling numbers* and four *wavelet numbers*. *Daub4* is capable of decomposing the original signal into *trend* and *fluctuation subsignals* and introducing *wrap-around effect* [35]. In general, the trend subsignal represents the localized lower frequency component of the original signal, whereas the fluctuation subsignal corresponds to the higher frequency component. In practice, *Daub4* is capable to be deemed as high- and low-pass filters with a cut-off frequency of $\omega_s/2^{K+1}$ Hz, where ω_s and K are the sampling frequency of signal measurement and level number of DWT, respectively [35]. When a measured thrust force signal f with N samples is given to K -level *Daub4*, the K -level trend subsignal (a_K) and K -level fluctuation subsignal (d_K) can be defined as shown in (1) and (3) [35].

$$a_K = (a_{K_1}, \dots, a_{K_l}, \dots, a_{K_{N_K}}); N_K = N/2^K \tag{1}$$

$$a_{K_l} = f \cdot V_{K_l} \tag{2}$$

$$d_K = (d_{K_1}, \dots, d_{K_l}, \dots, d_{K_{N_K}}) \tag{3}$$

$$d_{K_l} = f \cdot W_{K_l} \tag{4}$$

where a_{K_l} and V_{K_l} are the l th *scaling coefficients* and the l th K -level *scaling signals* [35] (also called *scaling functions* [36]) of *Daub4*, respectively. The scaling function V_{K_l} is composed of zeros and four scaling numbers. Similarly, d_{K_l} and W_{K_l} are the l th *wavelet coefficients* and the l th K -level *wavelet signals* of *Daub4*, respectively. The wavelet function W_{K_l} is composed of zeros and four *wavelet numbers*.

2.3 ANN

An ANN is constructed using back propagation algorithms to estimate flank wear in this study. As shown in Fig. 2, the ANN used in this study is composed of the three layers, namely, input, hidden, and output layers. Input and output layers may have multiple neurons. In this study, the number of input neurons was set two for two features corresponding to the quasi-static and dynamic components of the thrust force signal. The output layer has a single neuron corresponding to flank wear. The data for the two inputs and an output are normalized before applying to the ANN training process. Normalization of each input feature in this study is made according to (5) [27]

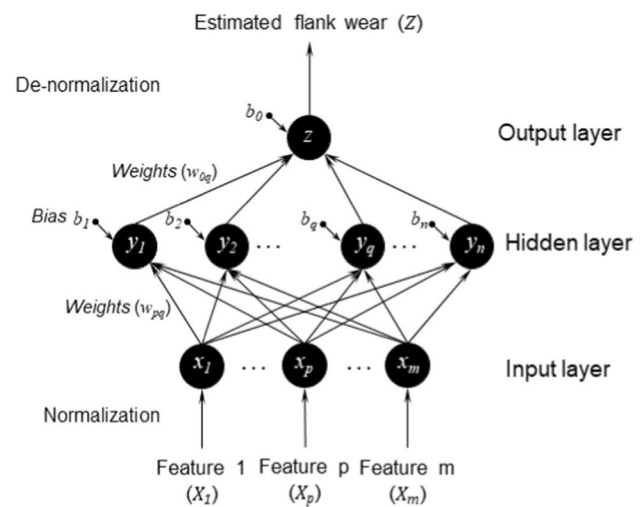


Fig. 2 ANN structure applied in this study

$$x = 2 \times (X - X_{min}) / (X_{max} - X_{min}) - 1 \tag{5}$$

where x and X are the values of the normalized and original input features, respectively. The maximum and minimum values of all the original input features engaged in the training process are X_{min} and X_{max} , respectively. As a result, all the normalized values of the extracted features would be distributed between -1 and 1 . As shown in Fig. 2, the value at each neuron in the upper layer (for example, y_q on the hidden layer) is defined as follows:

$$y_q = G \left(\left(\sum_{p=1}^m w_{pq} x_p \right) + b_q \right), \quad (1 \leq p \leq m, 1 \leq q \leq n) \tag{6}$$

where w_{pq} is the weight from neurons x_p (lower layer neuron) to y_q (upper layer neuron), which corresponds to the arrow shown in Fig. 2, whereas b_q is the bias for neuron y_q . G is the transfer function and the *hyperbolic tangent sigmoid function* [37] applied in this study. In addition, m and n are the numbers of neurons in the lower and upper layers, respectively. The output value of the neuron z can be obtained from (6) in the same way. The estimated flank wear could be calculated by denormalization, which is the inverse function of (5).

In this study, we have chosen a $2 \times 5 \times 1$ structure, which has two neurons in the input layer ($m=2$) and five neurons in the hidden layer ($n=5$). The initialized weight and bias are set as random numbers. Being trained by iterations, weights and biases would be increasingly suitable for estimation of flank wear. The training process was performed on MATLAB with the training function based on Levenberg–Marquardt algorithm.

3 Experiments

In this study, a computer numerical controlled (CNC) machining center (CSCAM, M643-T14-A3) was used in drilling CFRP samples. Thrust force signals were obtained from a 4-component tool dynamometer and its charge amplifier (Kistler, 9272 and 5070) with the help of an ADC (National Instruments, cDAQ-9174). The sampling frequency in signal measurement was set as 1,000 Hz. All the signal processing steps, including DWT and ANN, were performed in LabVIEW environment. Figure 3 shows the schematic diagram of experimental setup.

Solid spiral drilling tools with the same point angle and material but with two different diameters, namely, 8 mm and 6 mm, were used in the drilling experiments. The point angle of the tools was 118° . The tools were made of tungsten carbide (WC) without any surface coating. Figure 4a shows a new tool with a diameter of 8 mm. The CFRP workpiece was a multidirectional (MD) stack laminate with thickness of 5 mm, which was composed of epoxy resin and carbon fibers with a laying-up sequence of $0^\circ/45^\circ/90^\circ/-45^\circ$ orientation

(i.e., quadraxial). Moreover, a woven carbon fiber sheet was laid on the top and bottom layers. The carbon fibers were T1000 class. The CFRP workpieces were provided by an airplane company (Korea Aerospace Industries Ltd.). Figure 4b shows a CFRP plate workpiece used in this study. The feedrate and spindle speed were 400 mm/min and 5000 rpm, as recommended by the tool maker.

Each tool was used in drilling 500 holes (equivalent to 2500 mm in drilling length) on CFRP. The tool wear and thrust force signal were investigated at every 100 holes from the 50th hole and at the first and last hole drilling. The number of repetitions for 8-mm and 6-mm tools was 5 and 3, respectively. To measure the flank wear, a photo was taken for the flank face using a stereomicroscope (SMZ460, Nikon) with a charge coupled device (CCD) camera. The cutting edge of each tool was laid horizontally with the help of a tool holder designed with considering the point angle of the tools. The averaged flank wear (V_B) was calculated with the help of ImageJ software (National Institutes of Health). Only the flank wear along the cutting edge (or lip) was considered in this study.

Fig. 3 Schematic diagram of experimental setup

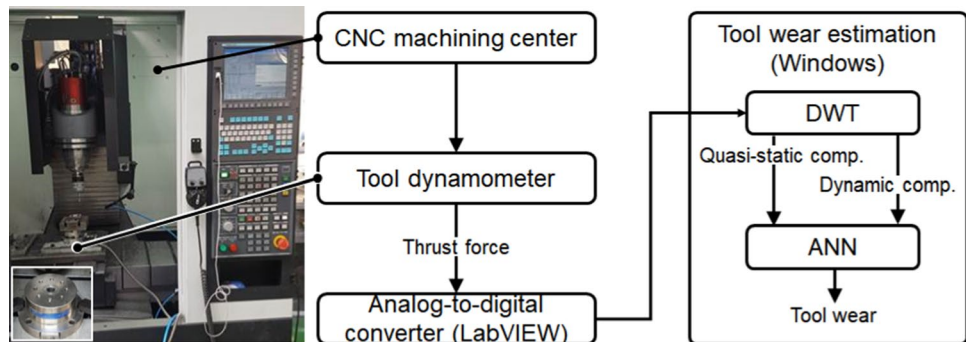


Fig. 4 Drilling tool and CFRP workpiece used in this study: **a** new tool (with a diameter of 8 mm) and **b** new CFRP workpiece

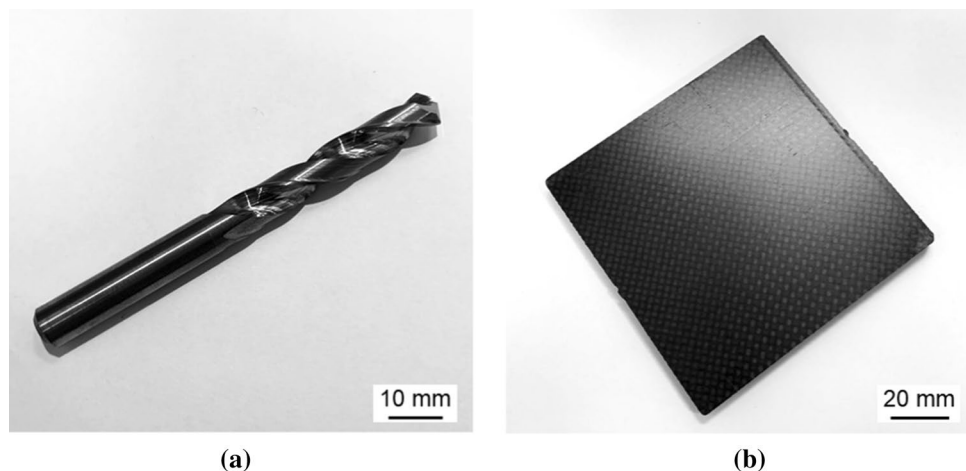


Fig. 5 Flank faces of tools with a diameter of 8 mm and top/bottom surfaces of workpieces: **a** and **d** fresh tool; **b** and **e** worn tool after drilling 1250 mm of CFRP (equivalent to 250 holes); and **c** and **f** worn tool after drilling 2500 mm of CFRP (equivalent to 500 holes). White arrows in (a–c) denote the flank wear on the flank face along the cutting edge

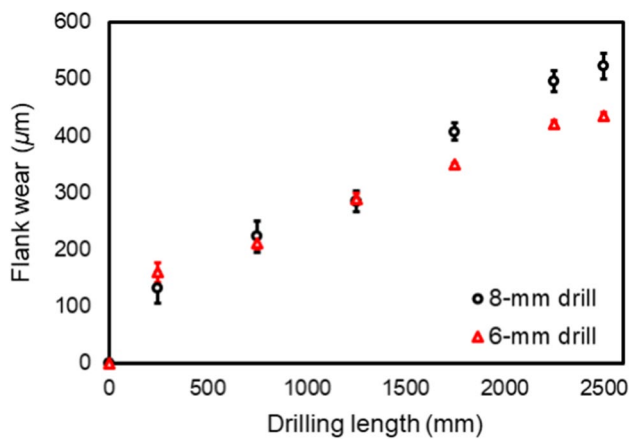
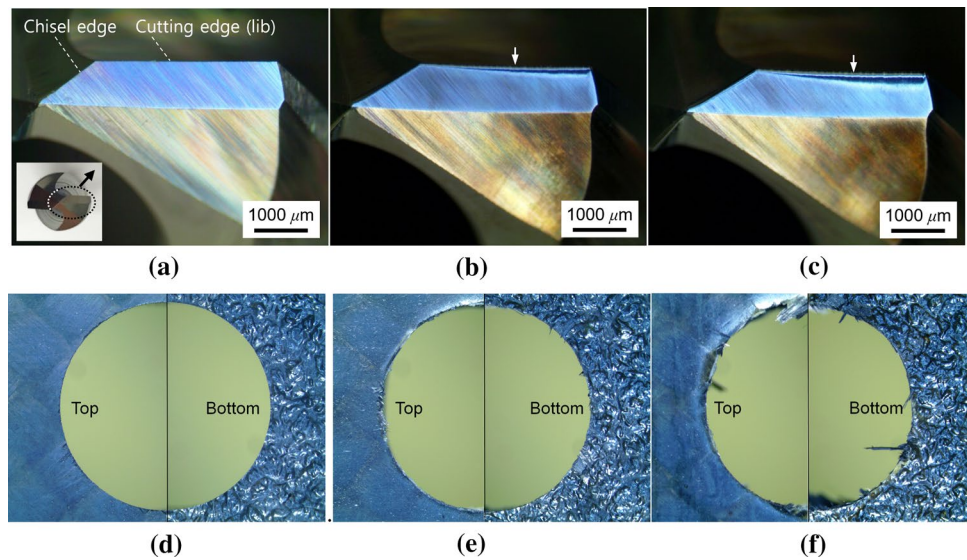


Fig. 6 Flank wear growth with respect to drilling length for 8-mm and 6-mm diameter tools

4 Results and Discussions

Figures 5a–c show the flank faces of the 8-mm tools after drilling CFRP for different lengths of 0, 1250, and 2500 mm. The edge of the flank face had changed evidently as much as it engaged in drilling CFRP. Specifically, the edge had larger flank wear as it was closer to its side end. The tool with a diameter of 6 mm showed a similar trend but with a slightly smaller magnitude in flank wear growth. Moreover, the machined holes corresponding to the tool conditions shown in Fig. 5a–c are presented in Fig. 5d–f. The hole machined using a fresh tool does not have any failure. However, the holes for the worn tools had various failures such as uncut resin, fibers, spalling, and delamination as shown in the figures. As expected, the failure became more severe with increased drilling length

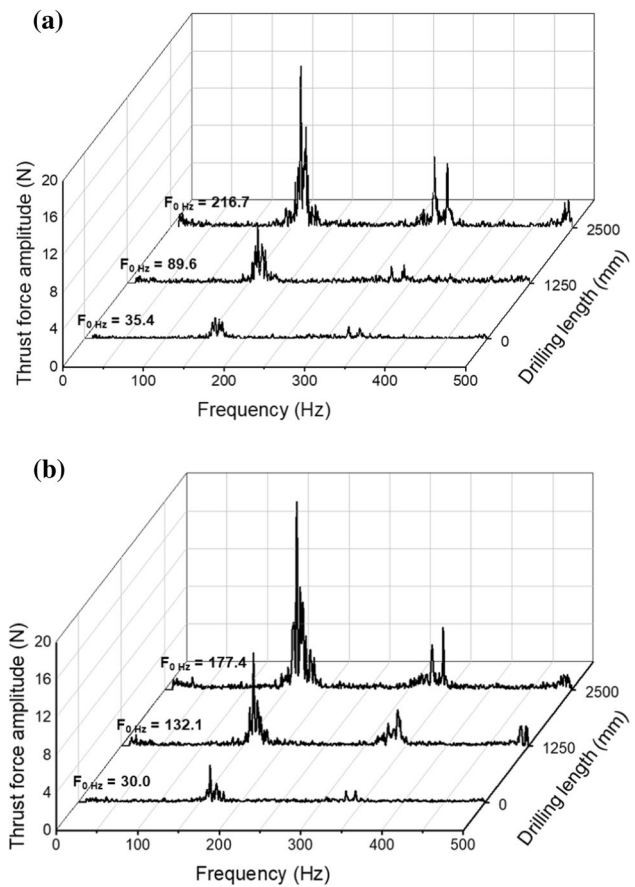


Fig. 7 FFT results of measured thrust force signals with respect to drilling length: **a** 8-mm tool and **b** 6-mm tool

(i.e., larger tool wear). The flank wear growth of the both tools with the diameters of 8 mm and 6 mm according to the drilling length is shown in Fig. 6. In particular,

the flank wear in both tool conditions grew faster when the tool machined holes up to initial 250 mm (or slightly longer) drilling, and then it became slightly slower.

Figure 7 shows the amplitude spectrums obtained from FFT for the thrust force signals when drilling CFRP 1250 mm using (a) 8-mm diameter and (b) 6-mm diameter tools. The frequency components lower than 10 Hz were cut out using high-pass filtering with a cut-off frequency of 10 Hz. However, the peak amplitude in the frequency range lower than 10 Hz was denoted as $F_{0\text{Hz}}$, given that the frequency corresponding to the peak amplitude was 0 Hz in all the experiments. It was also provided for each drilling length condition. As shown from the obtained values, the value of $F_{0\text{Hz}}$ had a strong relation to the drilling length. Thus, the value increased as the drilling length increased. Over the frequency range higher than 10 Hz, the dominant vibration components at the frequency near 166 Hz and its harmonics were observed. They were equivalent to a double spindle rotation frequency, that is the 2nd harmonic component of runout frequency. In this study, the frequency was called cutting-edge passing frequency. Figure 7 shows that the cutting-edge passing frequency component looked sensitive to the drilling length, which corresponds to the tool wear as shown in Figure 6. The drilling tool with longer drilling length (equivalently, larger tool wear) had a larger thrust force amplitude at the cutting-edge passing frequency. The second and higher-order harmonic components of the cutting-edge passing frequency were ignored due to their small amplitude. From these amplitude spectrum analyses, the typical quasi-static, which was $F_{0\text{Hz}}$, and the dynamic (at cutting-edge passing frequency) components of the thrust force signal were selected to estimate the tool wear in this study.

The static and dynamic components of the thrust force signal were obtained separately using DWT. In general, the frequency resolution and band size were determined using the level of DWT, which was strongly related to calculation load and the processing steps at the same time. Therefore, the level and subsignals of DWT suitable for the quasi-static and dynamic components of the thrust force were selected to minimize the calculation load and processing steps. The static component of thrust force could be represented as the frequency component within lower frequency. Thus, the level 5 scaling functions (a_5) were chosen to cover the quasi-static component of the thrust force, given that it was the corresponding frequency band of 0 to 15.625 Hz. Moreover, the dynamic component of thrust force was extracted using the level 2 wavelet functions (d_2) to indicate the vibratory behavior of the thrust force signal around the cutting-edge passing frequency as shown in Fig. 7. d_2 covered the frequency band between 125 and 250 Hz. Figure 8a shows the thrust force signal obtained when drilling a CFRP using an 8-mm diameter tool with a drilling length of 1250 mm.

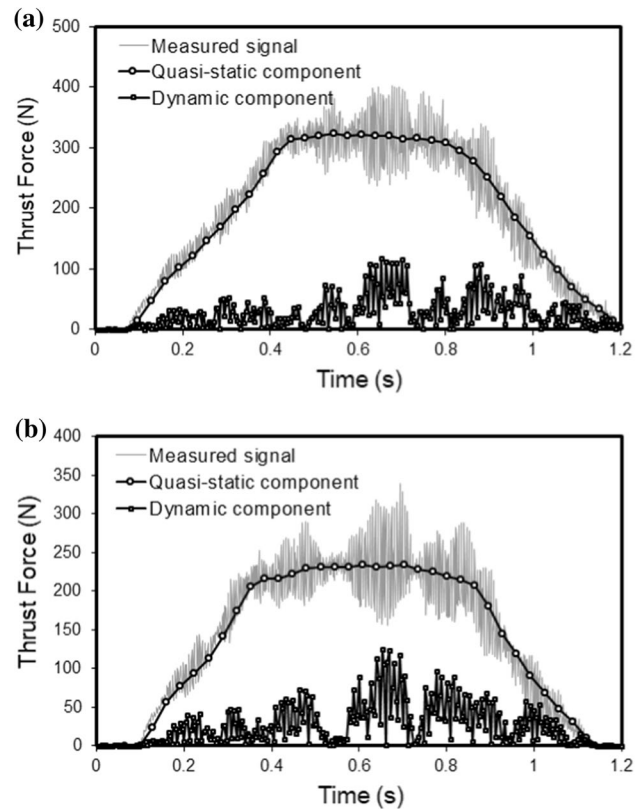


Fig. 8 DWT results for thrust force signal obtained when drilling CFRPs with different diameter tools: **a** 8 mm and **b** 6 mm

Its quasi-static and dynamic components are also obtained using DWT. As shown in Fig. 8b, the comparison of the measured thrust force signal and its quasi-static and dynamic components from DWT when a 6-mm diameter tool with the same drilling length was used. Furthermore, the quasi-static component obtained using DWT can effectively describe the change in the level of the original signal. The dynamic component also successfully represented the vibratory behavior of the original signal. The absolute value of level 2 wavelet functions ($|d_2|$) was used as the dynamic component of the thrust force for the purpose of easy extraction of amplitude information of the vibratory behavior.

As shown in Fig. 8, the quasi-static and dynamic components of thrust force went through significant changes in level during hole drilling. A measure (or representative value) for each component was useful in determining a relationship between the components and tool wear. In this study, the maximum values of quasi-static and dynamic components, namely, $\max(a_5)$ and $\max(|d_2|)$, were used as the measures. These values also played the role of the inputs to the ANN-based tool wear estimator. The correlations between the tool wear and maximum values of the quasi-static and dynamic components of the thrust force were investigated as shown in Fig. 9a–c.

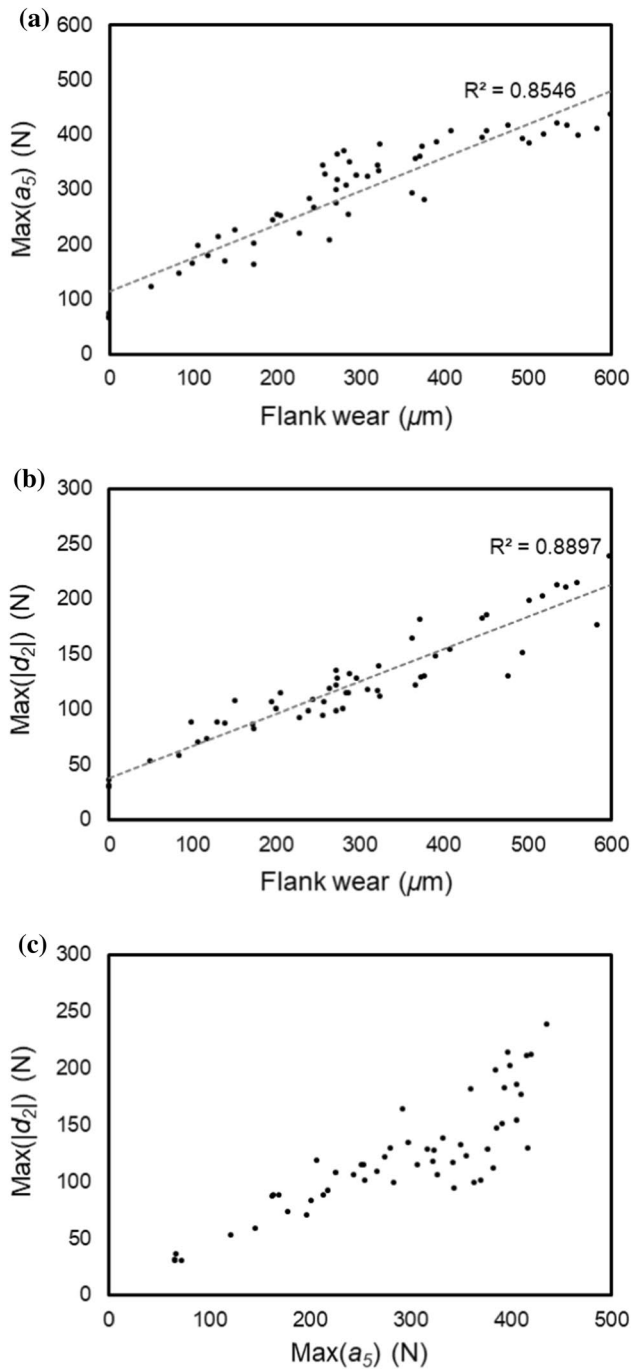


Fig. 9 Analysis results for correlation between **a** tool wear and maximum value of quasi-static component, **b** tool wear and maximum value of dynamic component, and **c** maximum values of quasi-static and dynamic components when drilling with 8-mm tools

As shown in Figures 9a–b, the quasi-static and dynamic components were highly proportional to tool wear. However, the variation was larger as the tool wear increased. Moreover, the correlation between the maximum values of the quasi-static and dynamic components was investigated as shown in Fig. 9c. A strong dependency with

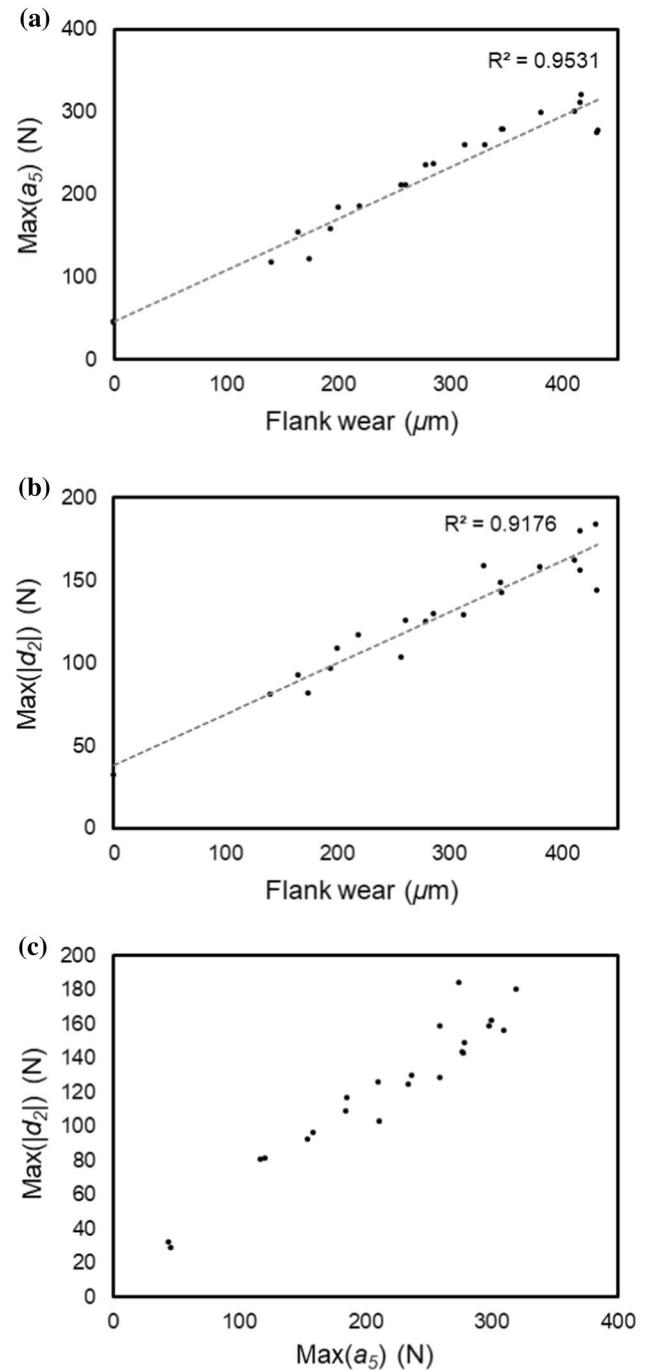


Fig. 10 Analysis results for correlation between **a** tool wear and the maximum value of quasi-static component, **b** tool wear and the maximum value of dynamic component, **c** the maximum values of quasi-static and dynamic components when drilling with 6-mm tools

each other was observed, where the Pearson correlation coefficient [38] was approximately 0.79. The correlation between the two values, $\text{max}(a_5)$ and $\text{max}(|d_2|)$, was relatively higher when their values were smaller. However, the correlation had worsened as the values became continually larger. These correlative properties of the quasi-static and

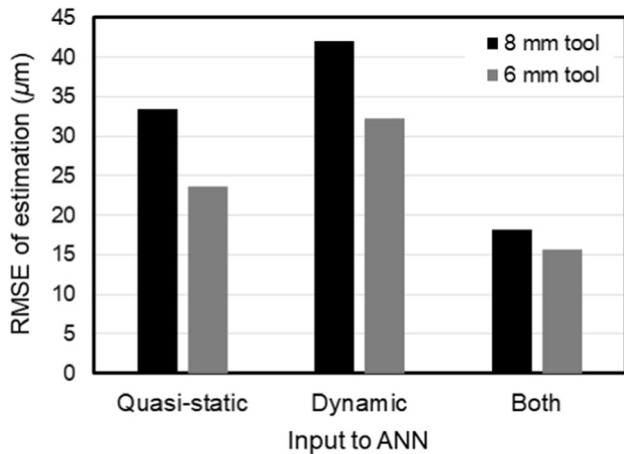


Fig. 11 Comparison of RMSE of DWT–ANN-based tool wear estimation using three sets of features, namely, maximum value of quasi-static component of thrust force only (single input), maximum value of dynamic component of thrust force only (single input), and both maximum values of quasi-static and dynamic components of thrust force separately (multiple inputs) when drilling using 8- and 6-mm diameter tools

dynamic components of the thrust force were shown similarly when drilling with 6-mm tools even though the correlations were slightly higher (Figure 10). Therefore, these two features need to be considered separately to estimate the tool wear accurately under a larger tool wear condition. As a result, $\max(a_5)$ and $\max(l_{d2})$ were used as the inputs to ANN in this study.

To justify the estimation of the tool wear using the selected two features, $\max(a_5)$ and $\max(l_{d2})$, we conducted three types of tool wear estimation. Specifically, the ANN-based tool wear estimation used each of the two features and both features as inputs. Figure 11 presents the comparison results of the root mean square errors (RMSE) in ANN training for the three types of tool wear estimation. As shown in Fig. 11, ANN with the two inputs had estimated flank wear more accurately than the other two methods based on single input in CFRP drilling with the 8-mm tools. The estimation error when using two inputs was less than 46% of that from quasi-static component only and approximately 57% of that in dynamic component-based estimation. Similarly, the wear estimation quality for 6 mm tool when both features were employed looked better than that of the other methods. In detail, the estimation error when using both features in the developed system was less than 34% of that from quasi-static component only and approximately 52% of that in dynamic component-based estimation. Thus, the use of quasi-static and dynamic components as independent inputs could improve the accuracy of the estimation of the tool wear, which was supposed to be originated from the complementary effect of both components. By contrast, single component input could additionally introduce erratic components caused by unexpected or undesired machining situations.

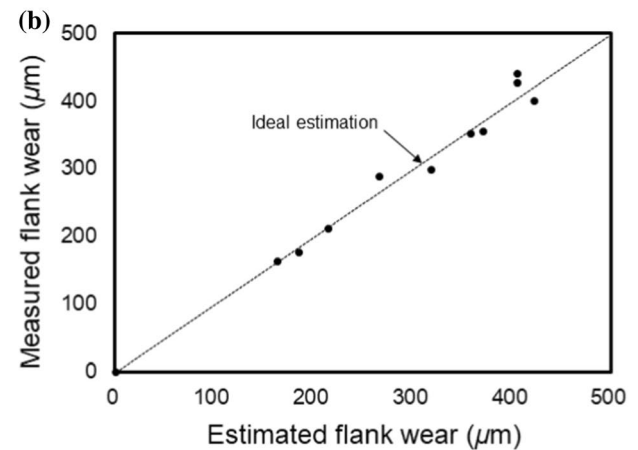
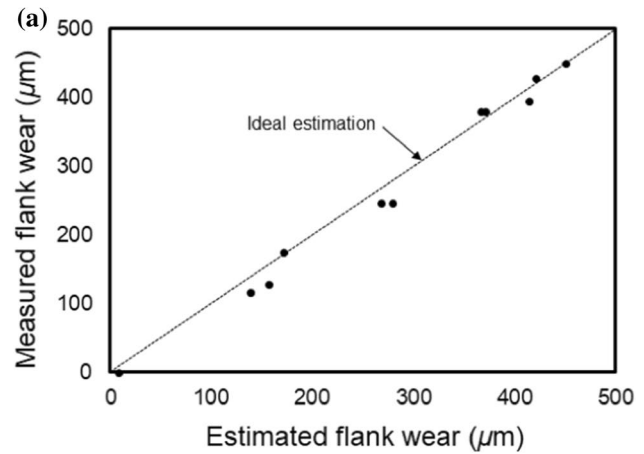


Fig. 12 Estimation results of tool wear in CFRP drilling. **a** Justification experiment 1 with an 8-mm diameter tool and **b** Justification experiment 2 with a 6-mm diameter tool

The developed tool wear estimation based on DWT and ANN with two thrust force component inputs was evaluated using the signals that were not engaged in ANN training. Figure 12a, b show the wear estimation results of the 8-mm and 6-mm diameter tools using the developed method, respectively. As shown in these figures, the tool wear of both tools was successfully estimated using the proposed method. The maximum estimation error for the 8-mm diameter tool was approximately 22%. This value corresponded to an error of 28.7 μm for the actual tool wear of 128 μm, and the average error was approximately 7.8%. Moreover, the maximum and average errors for the 6-mm diameter tool were approximately 8.1% and 4.4%, respectively.

5 Conclusions

In this study, a tool wear estimation based on DWT and ANN was successfully applied to CFRP drilling which has more significant tool wear but lower cutting loads. Drilling

tools with two different diameters and MD CFRP stack workpieces for a real aircraft were used in a series of experiments. Each tool was engaged in drilling 500 holes. From the experiments, the flank wear and thrust force with respect to the drilling length were investigated. In particular, the quasi-static and dynamic components of thrust force were selected as feature signals contrary to existing studies which typically used only quasi-static component from the various ones of thrust force. The quasi-static component covers the cutting force increase induced by the tool wear, whereas the dynamic component corresponds to the vibration rise caused by the tool wear. These two features had a strong relationship not only with the tool wear but also with each other. However, the dependency between the two features weakened as the tool wear increased. As a result, the two features effectively extracted using DWT were used as independent inputs to ANN. Consequently, our system based on DWT–ANN with two inputs could estimate more effectively with at least 34% less error than that with single input. Moreover, the maximum estimation error was approximately 22% and the average error was less than 8%.

Acknowledgements This work was supported by the Technology Innovation Program (10053248, Development of Manufacturing System for CFRP (Carbon Fiber Reinforced Plastics) Machining) funded By the Ministry of Trade, industry & Energy (MOTIE, Korea) and the National Research Foundation of Korea (NRF) grant funded by the Korea government (MSIT) (No. NRF-2020R1A4A1018652, 2021R1A2C2014364) and by the MSIT (Ministry of Science, ICT), Korea, under the High-Potential Individuals Global Training Program) (2020-0-01519) supervised by the IITP (Institute for Information & Communications Technology Planning & Evaluation).

References

- Che, D., Saxena, I., Han, P., Guo, P., & Ehmann, K. F. (2014). Machining of carbon fiber reinforced plastics/polymers: a literature review. *Journal of Manufacturing Science and Engineering*, 136(3), 034001.
- Wang, X., Kwon, P. Y., Sturtevant, C., & Lantrip, J. (2013). Tool wear of coated drills in drilling CFRP. *Journal of Manufacturing Processes*, 15(1), 127–135.
- Shaban, Y., Meshreki, M., Yacout, S., Balazinski, M., & Attia, H. (2017). Process control based on pattern recognition for routing carbon fiber reinforced polymer. *Journal of Intelligent Manufacturing*, 28(1), 165–179.
- Obradovic, J., Boria, S., & Belingardi, G. (2012). Lightweight design and crash analysis of composite frontal impact energy absorbing structures. *Composite Structures*, 94(2), 423–430.
- Smojver, I., & Ivančević, D. (2011). Bird strike damage analysis in aircraft structures using Abaqus/Explicit and coupled Eulerian Lagrangian approach. *Composites science and technology*, 71(4), 489–498.
- Meeks, C., Greenhalgh, E., & Falzon, B. G. (2005). Stiffener debonding mechanisms in post-buckled CFRP aerospace panels. *Composites Part A: Applied science and manufacturing*, 36(7), 934–946.
- Ye, L., Lu, Y., Su, Z., & Meng, G. (2005). Functionalized composite structures for new generation airframes: A review. *Composites science and technology*, 65(9), 1436–1446.
- Park, J.-M., Kwon, D.-J., Wang, Z.-J., Gu, G.-Y., & DeVries, K. L. (2013). Effect of thermal treatment temperatures on the reinforcing and interfacial properties of recycled carbon fiber–phenolic composites. *Composites Part A: Applied science and manufacturing*, 47, 156–164.
- Ren, L., Fang, Z., Wang, K. (2018). Design and behavior of super-long span cable-stayed bridge with CFRP cables and UHPC members. *Composites Part B: Engineering*, 164, 72–81.
- Calzada, K. A., Kapoor, S. G., DeVor, R. E., Samuel, J., & Srivastava, A. K. (2012). Modeling and interpretation of fiber orientation-based failure mechanisms in machining of carbon fiber-reinforced polymer composites. *Journal of Manufacturing Processes*, 14(2), 141–149.
- Iliescu, D., Gehin, D., Gutierrez, M., & Girot, F. (2010). Modeling and tool wear in drilling of CFRP. *International Journal of Machine Tools and Manufacture*, 50(2), 204–213.
- Rawat, S., & Attia, H. (2009). Wear mechanisms and tool life management of WC–Co drills during dry high speed drilling of woven carbon fibre composites. *Wear*, 267(5–8), 1022–1030.
- Faraz, A., Biermann, D., & Weinert, K. (2009). Cutting edge rounding: An innovative tool wear criterion in drilling CFRP composite laminates. *International Journal of Machine Tools and Manufacture*, 49(15), 1185–1196.
- Chen, W.-C. (1997). Some experimental investigations in the drilling of carbon fiber-reinforced plastic (CFRP) composite laminates. *International Journal of Machine Tools and Manufacture*, 37(8), 1097–1108.
- Teti, R. (2002). Machining of composite materials. *CIRP Annals-Manufacturing Technology*, 51(2), 611–634.
- Abhishek, K., Kumar, V. R., Datta, S., & Mahapatra, S. S. (2017). Parametric appraisal and optimization in machining of CFRP composites by using TLBO (teaching–learning based optimization algorithm). *Journal of Intelligent Manufacturing*, 28(8), 1769–1785.
- Hocheng, H., & Puw, H. (1992). On drilling characteristics of fiber-reinforced thermoset and thermoplastics. *International Journal of Machine Tools and Manufacture*, 32(4), 583–592.
- Islam, M. M., Li, C. P., & Ko, T. J. (2017). Dry electrical discharge machining for deburring drilled holes in CFRP composite. *International Journal of Precision Engineering and Manufacturing-Green Technology*, 4(2), 149–154.
- Lin, S., & Chen, I. (1996). Drilling carbon fiber-reinforced composite material at high speed. *Wear*, 194(1–2), 156–162.
- Hou, G., Qiu, J., Zhang, K., Cao, S., Cheng, H., Luo, B., & Cheng, Y. (2020). Comparative tool wear and hole quality investigation in drilling of aerospace grade T800 CFRP using different external cooling lubricants. *The International Journal of Advanced Manufacturing Technology*, 106(3), 937–951.
- Dalle Mura, M., & Dini, G. (2021). Drilling carbon fiber reinforced plastics with pre-cooling treatment by cryogenic fluid. *Journal of Manufacturing Processes*, 68, 23–31.
- Byrne, G., Dornfeld, D., Inasaki, I., Ketteler, G., König, W., & Teti, R. (1995). Tool condition monitoring (TCM)—the status of research and industrial application. *CIRP Annals-Manufacturing Technology*, 44(2), 541–567.
- Jantunen, E. (2002). A summary of methods applied to tool condition monitoring in drilling. *International Journal of Machine Tools and Manufacture*, 42(9), 997–1010.
- Chao, P. Y., & Hwang, Y. D. (1997). An improved neural network model for the prediction of cutting tool life. *Journal of Intelligent Manufacturing*, 8(2), 107–115.
- Caggiano, A., & Nele, L. (2018). Artificial neural networks for tool wear prediction based on sensor fusion monitoring of

CFRP/CFRP stack drilling. *International Journal of Automation Technology*, 12(3), 275–281.

26. Al-Sulaiman, F. A., Baseer, M. A., & Sheikh, A. K. (2005). Use of electrical power for online monitoring of tool condition. *Journal of Materials Processing Technology*, 166(3), 364–371.
27. Khashaba, U., El-Sonbaty, I., Selmy, A., & Megahed, A. (2010). Machinability analysis in drilling woven GFR/epoxy composites: Part II—Effect of drill wear. *Composites Part A: Applied science and manufacturing*, 41(9), 1130–1137.
28. Liu, D., Tang, Y., & Cong, W. (2012). A review of mechanical drilling for composite laminates. *Composite Structures*, 94(4), 1265–1279.
29. Arul, S., Vijayaraghavan, L., & Malhotra, S. (2007). Online monitoring of acoustic emission for quality control in drilling of polymeric composites. *Journal of Materials Processing Technology*, 185(1–3), 184–190.
30. Zhu, G., Hu, S., & Tang, H. (2021). Prediction of tool wear in CFRP drilling based on neural network with multicharacteristics and multisignal sources. *Composites and Advanced Materials*, 30, 2633366X20987234.
31. Zhang, Y., Wu, D., & Chen, K. (2019). A theoretical model for predicting the CFRP drilling-countersinking thrust force of stacks. *Composite Structures*, 209, 337–348.
32. Rimpault, X., Chatelain, J.-F., Klemberg-Sapieha, J., & Balazinski, M. (2017). Tool wear and surface quality assessment of CFRP trimming using fractal analyses of the cutting force signals. *CIRP Journal of Manufacturing Science and Technology*, 16, 72–80.
33. Zhu, K., San Wong, Y., & Hong, G. S. (2009). Wavelet analysis of sensor signals for tool condition monitoring: A review and some new results. *International Journal of Machine Tools and Manufacture*, 49(7–8), 537–553.
34. Mallat, S. (1999). *A wavelet tour of signal processing*. Elsevier.
35. Walker, J. S. (2002). *A primer on wavelets and their scientific applications*. CRC Press.
36. Mallat, S. G. (1989). A theory for multiresolution signal decomposition: The wavelet representation. *IEEE Transactions on Pattern Analysis Machine Intelligence*, 7, 674–693.
37. Laudani, A., Lozito, G. M., Fulginei, F. R., & Salvini, A. (2015). On training efficiency and computational costs of a feed forward neural network: A review. *Computational intelligence and neuroscience*, 2015, 83.
38. Benesty, J., Chen, J., Huang, Y., & Cohen, I. (2009). *Noise reduction in speech processing*. Springer.

Publisher's Note Springer Nature remains neutral with regard to jurisdictional claims in published maps and institutional affiliations.



Chengwen Han is a freelance data analyst in China. He received his MS degree in Mechanical Engineering from Kyungpook National University, Daegu, Korea. His research interests include manufacturing process monitoring and automation.



Kyeong Bin Kim is a Team Leader in Technology Center, Seon Jin Precision Co. Ltd., Daegu, Korea. He received his MS degree in Mechanical Engineering from Kyungpook National University, Daegu, Korea. His research interests include machining process monitoring and advanced materials manufacturing.



Seok Woo Lee is an Executive Managing Director of Research Institute of Clean Manufacturing System, Korea Institute of Industrial Technology, Cheonan, Korea. He received his Ph.D. in Mechanical Engineering from Pusan National University, Pusan, Korea. His research interests include advanced materials manufacturing and robot machining.



Martin Byung-Guk Jun is an Associate Professor in School of Mechanical Engineering, Purdue University. He received his Ph.D. degree in Mechanical Engineering from University of Illinois at Urbana-Champaign, Urbana, USA. His research interests are smart manufacturing and micro-manufacturing processes.



Young Hun Jeong is an Associate Professor of the School of Mechanical Engineering, Kyungpook National University, Daegu, Korea. He received his Ph.D. degree in Mechanical Engineering from POSTECH, Pohang, Korea. His research interests include precision machining, nano/micro manufacturing and biomaterials.